Simulation study of the evolution mechanisms of clusters in a large-scale liquid Al system during rapid cooling processes

Simulation study of the evolution mechanisms of clusters in a large-scale liquid Al system during rapid cooling processes

K J Dong[1,2]**, R S Liu**[2]**, A B Yu**[1]**, R P Zou**[1] **and J Y Li**[2]

[1] School of Materials Science and Engineering, The University of New South Wales, Sydney, New South Wales 2052, Australia
[2] Department of Physics, Hunan University, 410082, People's Republic of China

E-mail: rsliu@hnu.net.cn or liurangsu@sina.com

Abstract

Molecular dynamics simulations have been performed for a large-scale system consisting of 400 000 atoms of liquid metal Al. To describe the complex microstructural evolutions in the liquid system during the rapid cooling processes, the tracing atom method and cluster bond-type index method have been used. It is demonstrated that the number of (12 0 12 0) icosahedral clusters, consisting of the 1551 bond type, with a higher degree of ordering, increases continuously and plays a critical and leading role in the solidifying transition. Various cluster configurations, formed by icosahedral clusters and Frank–Kasper, Bernal and defective polyhedra, produce the short-range-order regions in this amorphous system, while the atoms not taking part in forming clusters give the sparse regions possessing disorder characteristics. Large cluster configurations consisting of more than 150 atoms have been found and are shown to be formed by combining smaller clusters and to be different from those obtained by gaseous deposition and ionic spray methods.

1. Introduction

Amorphous and microcrystalline metals and alloys prepared by rapid cooling processes have various excellent properties such as high strength, good soft magnetism and so on, and their macroscopic properties are mainly determined by microstructures. In order to develop effective methods to control the properties, it is very important to understand the evolution mechanisms of microstructure in forming amorphous and microcrystalline metals, but at this stage of development it is difficult to do so experimentally. This difficulty, however, can be overcome by using molecular dynamics simulation. Particularly, in recent years, as a result of the rapid development of computer technology, some steady progress has been made in this direction [1–12]. However, previous studies are often concerned with a system with a small number of atoms, e.g. 500–1000 atoms for liquid Al metal. Consequently, only small clusters can be

studied, and the results are not rich enough to understand the evolution of large clusters that may play an important role in the formation of amorphous and microcrystalline metals.

To be able to simulate reasonably a system containing nano-scale clusters, the number of atoms used in a MD simulation should be at least in the range of 10^5–10^6, and this is difficult to achieve with conventional sequential computers. With the newly developed parallel computational technique, it is now possible to perform such a large-scale simulation [13–15]. By the use of this technique, 50 000–100 000 Al atoms have been used in our previous MD simulations which can produce clusters containing more than 100 atoms [16, 17].

In recent years, there has been an increasing interest in various cluster structures of metals and non-metals because of their important applications in science and industry. But the studies thus far are mainly focused on the clusters formed by gaseous deposition and ionic spray methods [18–20], and to the authors' knowledge no work has been done on large clusters formed during cooling and solidification processes in liquid metallic systems. These large clusters may play an important role in the microstructural evolution of liquid metallic systems during rapid cooling processes. The purpose of this paper is to present a simulation study to clarify this issue by means of molecular dynamics and a parallel algorithm. In particular, it is focused on the evolution mechanisms of clusters in a large-scale liquid system consisting of 400 000 Al atoms during rapid cooling processes.

2. Simulation conditions

The conditions for the present simulation calculation are as follows. Firstly, 400 000 Al atoms are randomly placed in a cubic box. The task for their calculation is distributed among 40 computers by using a parallel algorithm. Then the system runs under periodic boundary conditions. The interacting interatomic potential adopted is the effective pair potential function developed based on the generalized energy independent non-local model pseudopotential [21, 22], given as

$$V(r) = (Z_{eff}^2/r)\left[1 - \left(\frac{2}{\pi}\right)\int_0^\infty dq \, F(q)\sin(rq)/q\right], \tag{1}$$

where Z_{eff} and $F(q)$ are, respectively, the effective ionic valence and the normalized energy wavenumber characteristic, as detailed elsewhere [21, 22]. This pair potential has a cut-off at 20.0 au (atomic units), as shown in figure 1. The time step chosen is 5.95×10^{-15} s. The cooling rate is 33.5×10^{12} K s^{-1}. The initial temperature is 943 K (the melting point of Al is 933 K).

In a simulation, the system first runs for 300 steps at 943 K to produce a quasi-equilibrium state which is reached when the system energy has no obvious change; such a state can be obtained after about 150 steps under the present simulation conditions. Second, the temperature of the system is gradually decreased, at the above given cooling rate, to a sequence of given temperatures: 883, 833, 780, 730, 675, 625, 550, 500, 400 and 300 K. The structural configurations of the system, i.e. the space coordinates of atoms, are recorded at each given temperature. Finally, the bond types between related atoms are detected by means of the index method of Honeycutt and Andersen (HA) [23], and the clusters formed are identified by a new method described in section 3.2.

3. Results and discussion

The validity of the proposed simulation is often verified by comparing the calculated pair distribution function $g(r)$ with the experimental results in the literature. This approach has
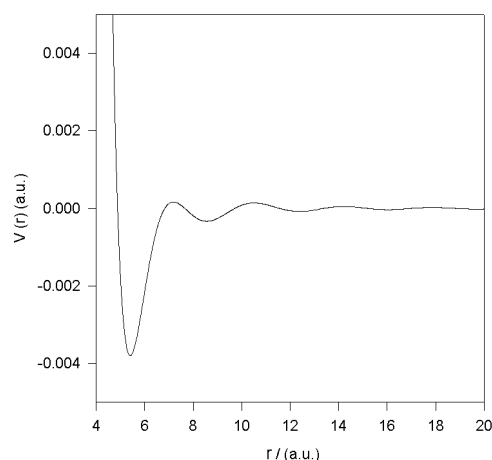
Figure 1. Effective pair potential $V(r)$ of liquid metal Al at 943 K.
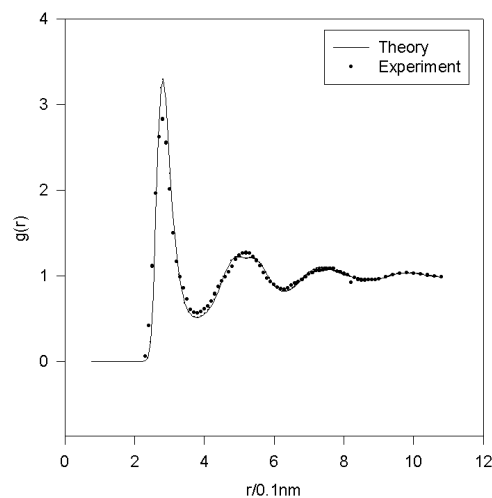

Figure 2. Pair distribution function $g(r)$ of liquid metal Al at 943 K.

also been employed in this work. Figure 2 shows the comparison between the present simulated results and the experimental results of Waseda [24]. Good agreement between the calculated and measured $g(r)$ is obvious. Moreover, figure 3 shows the $g(r)$ curves as a function of temperature. It can be seen from this figure that the second peaks of $g(r)$ become more explicit as temperature decreases, an important feature of amorphous metals and alloys. Therefore, the results in figures 2 and 3 confirm the effectiveness and accuracy of the simulation algorithm developed. On this basis more detailed analysis can be performed to understand the evolution of microstructures and the formation of clusters as described below.

3.1. Bonding relation

The bonding relations between atoms in the system can be described by using the bond-type index method of HA [23]. Figure 4 shows the main HA bond-type indices related to the
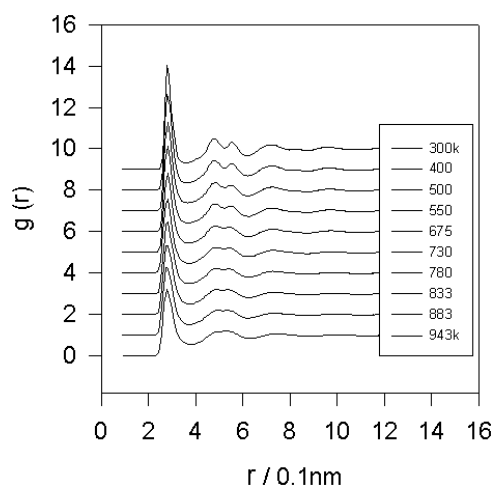
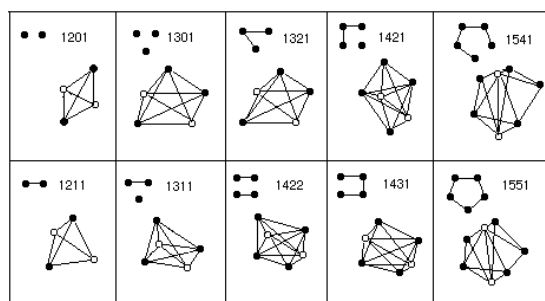**Figure 3.** Pair distribution functions $g(r)$ of liquid, supercooled and solid state Al (943–300 K).

Figure 4. Schematic diagrammatic nomenclature and configurations of HA indices.

present analysis. In this figure, white circles represent atoms in the pair of interest (under the considered 'root pair'), while black circles represent near-neighbour atoms belonging to both of the two white-circled atoms. Applying these HA indices to the present results, the relative bonding numbers at the considered temperatures are shown in table 1. The following results can be obtained from the analysis of this table.

- The relative numbers of 1551 and 1541 bond types, related to the icosahedral configuration, have respectively occupied 16.3 and 13.9% of bonds at 943 K, i.e., the two bond types represent 30.2% of the total number of all bond types. The relative number of the 1551 bond type is increased remarkably with decreasing temperature, reaching 29.0% at 300 K. In contrast, the relative number of the 1541 bond type is only slightly increased to 14.8 at 300 K. Although the values of these bond types differ from those found in our previous studies, they confirm that the 1551 bond type plays a dominant role in the evolution process of microstructures.
- The relative numbers of 1441, 1431, 1421 and 1422 bond types, related to the tetrahedral structures, represent, respectively, 4.4, 21.7, 3.3 and 7.0% of bonds at 943 K. Their sum amounts to 36.4% of the total number of all bond types, but decreases slowly with decreasing temperature to 32.3% at 300 K.

Table 1. Relations of the numbers of various bond types (%) to temperatures (K).

Temper-ature (K)	Bond types and corresponding relative numbers (%)													
	1201	1211	1301	1311	1321	1331	1421	1422	1431	1441	1541	1551	1661	1771
943	1.4	1.3	0.9	6.7	6.7	0.5	3.3	7.0	21.7	4.4	13.9	16.3	4.8	0.1
883	1.3	1.2	0.9	6.4	6.5	0.5	3.2	6.8	21.6	4.5	14.1	17.2	4.9	0.1
833	1.1	1.1	0.8	6.0	6.2	0.5	3.1	6.6	21.6	4.5	14.3	18.5	5.2	0.1
780	1.0	1.0	0.7	5.6	5.8	0.4	3.0	6.4	21.5	4.5	14.5	20.0	5.4	0.1
730	0.9	0.9	0.7	5.4	5.7	0.4	2.9	6.2	21.3	4.6	14.6	20.7	5.6	0.1
675	0.8	0.9	0.6	5.0	5.4	0.4	2.7	5.9	21.1	4.6	14.7	22.11	5.8	0.1
625	0.8	0.8	0.6	4.8	5.3	0.4	2.7	5.9	21.2	4.4	14.7	23.1	5.8	0.1
550	0.7	0.8	0.6	4.6	5.1	0.3	2.6	5.7	21.0	4.3	14.9	25.0	5.8	0.1
500	0.8	0.8	0.5	4.5	5.1	0.3	2.5	5.6	21.1	4.2	14.9	25.8	5.8	0.1
400	0.7	0.8	0.5	4.3	5.1	0.3	2.4	5.4	20.9	3.9	14.9	27.8	5.7	0.0
300	0.7	0.9	0.5	4.2	5.2	0.2	2.3	5.3	21.0	3.7	14.8	29.0	5.5	0.0

- The relative numbers of 1331, 1321, 1311 and 1301 bond types, related to the rhombohedral structures, all decrease with decreasing temperature, and their total number is reduced from 14.8% at 943 K to 10.1% at 300 K.
- The relative number of the 1661 bond type, related to hexahedral and bcc structures, does not change much, and is only about 4.8–5.5%.
- The relative numbers of 1201 and 1211 bond types, existing in nearly free states, decrease with decreasing temperature. Their total relative number is 3.1% at 943 K and down to 1.7% at 300 K.
- It is known that the 1771 bond type exists only in liquid and supercooled liquid states above 500 K, and disappears below 500 K (the glass transition temperature of Al [25]) in the solid state. This result has also been observed in the present simulation.

Notably, the total number of the bond types listed in table 2 is about 88.0% at 943 K and 93.3% at 300 K, so that, even at lower temperature, about 7% of HA bonds still do not belong to the listed bond types which represent the various types of short-range order. This result indicates that more than 88% of atoms will be in the structures with different degrees of ordering, and the number of atoms in the free state is no less than 7%, no matter whether the system is in liquid, supercooled liquid or solid amorphous states.

3.2. Cluster formation

The clusters of different sizes, formed with different kinds and numbers of HA bond types in the disordered systems, are very difficult to describe by the methods commonly used at present. Therefore, we here proposed a new cluster bond-type index method (CBTIM) using four integers to describe some important kinds of cluster, especially the larger clusters having more than 100 atoms. This method is based on the work of Qi and Wang [26] who successfully expressed the Frank–Kasper (FK) polyhedron, the Bernal polyhedron and other defective icosahedra. The meanings of the four integers used in the CBTIM are as follows. The first integer represents the number of surrounding atoms, which along with a central atom form a cluster. The second, third and fourth integers represent the numbers of 1441, 1551 and 1661 bond types, respectively, by which the surrounding atoms are connected with the central atom of the cluster. For example, (12 0 12 0) expresses an icosahedron that is composed of 13 atoms (one is the central atom, coordination number $Z = 12$) connected with twelve 1551 bond

Table 2. Variation of the number of clusters with temperature (K).

| Types of cluster	943	883	833	780	730	675	625	550	500	400	300
(12 0 10 2)	0	1	0	0	0	0	0	0	1	0	0
(12 0 12 0)	1362	1674	2248	2956	3323	4179	4843	6569	7358	9722	11 597
(14 0 12 2)	106	107	164	222	236	300	375	407	399	511	505
(15 0 12 3)	38	34	67	71	75	98	109	132	153	153	177
(16 0 12 4)	8	12	8	15	19	15	19	20	17	26	38
(17 0 12 5)	1	0	1	1	2	0	0	1	0	2	1
(16 1 8 6)	0	0	0	0	0	0	0	0	0	1	0
(17 1 8 7)	0	0	0	0	0	0	0	0	1	0	0
(14 1 10 2)	949	1124	1317	1653	1837	2252	2377	2859	3138	3471	3765
(14 1 10 3)	288	318	398	475	528	618	696	846	930	1054	1113
(15 1 10 4)	130	98	167	208	215	270	290	321	373	437	499
(16 1 10 5)	23	34	32	25	36	45	49	49	72	69	68
(17 1 10 6)	0	2	1	2	5	3	3	2	1	1	0
(12 2 6 4)	0	0	0	0	0	0	1	0	0	0	0
(14 2 6 6)	0	0	0	0	0	0	0	0	1	0	0
(10 2 8 0)	7	4	4	5	3	1	4	2	2	0	0
(11 2 8 1)	120	126	112	121	117	99	102	88	84	47	45
(12 2 8 2)	489	568	606	695	749	774	818	871	867	781	748
(13 2 8 3)	205	222	256	348	323	426	390	470	406	449	421
(14 2 8 4)	390	445	597	682	710	951	966	1159	1178	1306	1369
(15 2 8 5)	102	120	156	202	234	272	230	307	346	421	403
(16 2 8 6)	15	12	17	33	34	26	30	45	41	55	49
(17 2 8 7)	1	0	0	3	1	0	5	5	2	0	0
(13 3 4 6)	0	0	0	1	1	0	0	1	0	0	0
(10 3 6 1)	1	5	7	2	1	4	0	1	0	0	0
(11 3 6 2)	12	12	15	8	4	3	7	7	7	5	0
(12 3 6 3)	122	131	143	136	148	145	144	110	101	77	69
(13 3 6 4)	497	545	601	663	746	892	787	909	768	761	678
(14 3 6 5)	177	188	244	296	298	319	358	381	385	388	413
(15 3 6 6)	53	56	71	91	89	122	129	147	134	104	160
(16 3 6 7)	6	3	7	2	9	7	13	7	14	8	12
(17 3 6 8)	0	0	1	3	0	1	2	1	0	1	0
(10 4 4 2)	0	1	0	0	0	0	1	0	0	0	0
(11 4 4 3)	6	3	8	9	4	7	5	0	6	2	0
(12 4 4 4)	41	31	30	41	52	57	35	31	32	19	15
(13 4 4 5)	51	61	65	52	66	66	56	52	69	48	27
(14 4 4 6)	100	103	108	154	137	156	137	161	156	125	110
(15 4 4 7)	34	23	26	24	31	32	46	47	35	43	52
(16 4 4 8)	2	1	5	5	2	3	6	2	2	5	3
(12 5 2 5)	2	4	1	5	3	2	2	3	3	2	1
(13 5 2 6)	8	11	14	10	6	13	12	16	12	8	6
(15 5 2 8)	2	0	3	3	6	4	2	2	2	0	1
(16 5 2 9)	0	0	0	0	0	1	1	1	1	1	1
(14 6 0 8)	3	6	4	4	3	1	2	3	6	2	0
Total number of all clusters	5349	6085	7504	9226	10 053	12 164	13 052	16 035	17 103	20 126	22 347
Icosahedrons expressed by (12 0 12 0) related to the total numbers of all clusters (%)	25.46	27.51	29.96	32.04	33.05	34.36	37.11	40.97	43.03	48.36	51.90
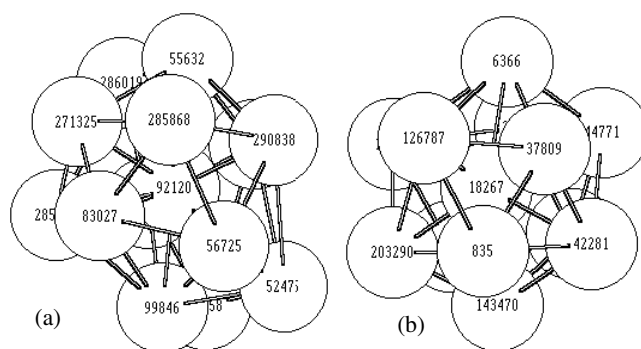
Figure 5. Schematics of icosahedron and defective icosahedron at 300 K. (a) An icosahedron (12 0 12 0) with the centre atom numbered as 18 267. (b) A defective icosahedron (13 1 10 2) with the centre atom numbered as 92 120.

types; (13 1 10 2) expresses the defective icosahedron composed by 14 atoms (coordination number $Z = 13$) connected with one 1441, ten 1551 and two 1661 bond types, as shown in figures 5(a) and (b), respectively. According to the CBTIM, we have obtained, for the present simulated results, the statistical numbers of various types of cluster related to icosahedra, defective icosahedra, FK and Bernal polyhedra, as listed in table 2. The analysis of the results in table 2 produces the following points.

- The number of icosahedra expressed by (12 0 12 0), with coordination number $Z = 12$, increases sharply from 1362 at 943 K to 11 597 at 300 K and occupies from 25.46 to 51.90% of the total number of clusters. The icosahedral clusters therefore play the most important role in the microstructure transition during the rapid cooling processes. The second important cluster is the defective icosahedron expressed as (13 1 10 2), with coordination number $Z = 13$; it numbers from 949 at 943 K to 3765 at 300 K, representing 17.74–16.85% of the total number of clusters. The other important defective icosahedra, in order of relative importance, are clusters (14 2 8 4), (14 1 10 3), (12 2 8 2) and (13 3 6 4).

- The number of canonical FK polyhedra expressed as (14 0 12 2), with coordination number $Z = 14$, is much less than that of the icosahedra but more than other defective FK polyhedra such as (15 0 12 3), (16 0 12 4) and (17 0 12 5). Especially, the polyhedron of (17 0 12 5) only appears once or twice at some temperatures.

- The number of canonical Bernal polyhedra expressed as (10 2 8 0) with coordination number $Z = 10$ only appears once or twice at some temperatures. However, the numbers of other defective Bernal polyhedra, as named in this work, are almost more than that of (11 2 8 5) whose coordination number is 11. Especially, the numbers of (12 2 8 2), (13 2 8 3), (14 2 8 4) and (15 2 8 5) are all more than 100 during all the cooling processes.

- It is of interest to note that the third integer of clusters, namely the number of the 1551 bond type in a cluster, can only be even numbers (12, 10, 8, 6, 4, 2, 0). The second and fourth integers, namely the 1441 and 1661 bond types, can be even and odd numbers (0, 1, 2, 3, 4, 5, 6, 7, 8, 9).

Why are various clusters formed with different ratios of 1441, 1551 and 1661 bond types so different in the number of clusters? The main reason must be their energies and the geometric configurations to be formed by these bond types. Some cluster configurations have lower energy and can be conveniently formed by combining 1441, 1551 and 1661 bond types with some suitable rates, and other types of cluster are difficult to form with these bond types.
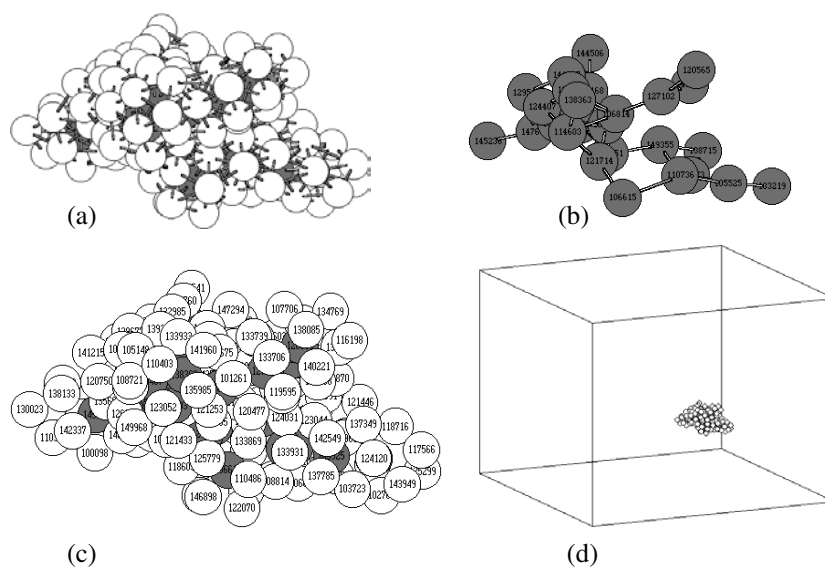
Figure 6. A larger cluster consisting of 150 atoms within 27 polyhedra at 400 K (composed of 7 icosahedra (12 0 12 0), 8 defective icosahedra (1(13 1 10 2), 6(14 1 10 3), 1(15 1 10 4)), 5 defective Bernal polyhedra (2 (14 2 8 4), 3(16 2 8 6)) and 7 defective polyhedra (1(12 3 6 3), 2(13 3 6 4), 1(14 3 6 5), 2(15 3 6 7)), 1(16 5 2 9). (a) schematic of cluster in whole view with bonding; (b) schematic of centre atoms in cluster with bonding; the cluster with labels; (d) the location of the cluster in the original box.

Therefore, up to now, we have only found 44 cluster types, of which some clusters appear once or twice in all the simulations performed, as listed in table 2.

Based on this observation, it is considered that the number of cluster types that can be formed in the liquid metal system during the cooling processes is limited and can satisfactorily be described by some rules as shown in table 2. This finding is important as it implies that it is possible to quantitatively describe the complicated microstructures in liquid and amorphous states by use of limited cluster types. We will discuss these rules in detail in the near future.

In this simulation, some larger clusters at a nano-cluster level have been found. These larger clusters are composed of various kinds of smaller cluster, and their size and amount increase with decreasing temperature. Their configurations are very complex. For example a large cluster consisting of 150 atoms is composed of 27 polyhedra with centre atoms (represented by grey circles), as shown in figure 6. From figures 6(a) and (b), it can be seen that a large cluster is produced by combining three different small clusters, and each small cluster composed of some polyhedra, and each polyhedron described by a set of indices in CBTIM. Interestingly the large clusters formed by rapid cooling from liquid Al metal do not consist of multi-shell configurations accumulated by atoms as obtained by gaseous deposition or ionic spray methods. The cluster configurations of Al formed by gaseous deposition have been verified by mass-spectrometer to be crystals or near crystals formed by octahedral shell structures [27, 28]. Therefore, different methods may produce different cluster configurations. From figure 6(c), it can be seen that the atoms contained in the cluster are labelled randomly; namely, the atoms in the system are distributed homogeneously. Figure 6(d), on the other hand, demonstrates that all the atoms in the large cluster are within the original box of the simulation, i.e., the large cluster is not outside the periodical boundaries. Therefore, clusters of various types can be generated in the present simulation under different conditions, as is the case in reality.
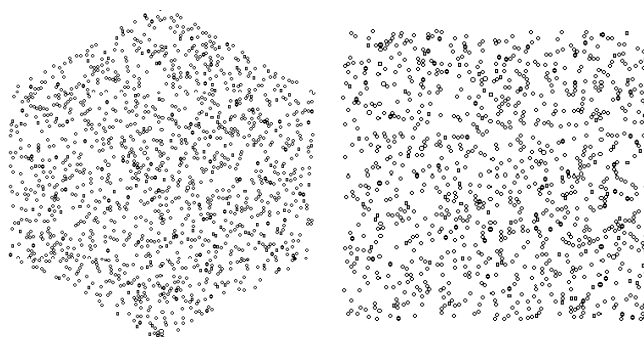
Figure 7. A 2D schematic diagram of the whole system consisting of 400 000 atoms at 300 K: (a) in (111) cross section; (b) in (100) cross section.

In general, the amorphous structures formed by rapid cooling from liquid metal Al are composed of two types of region as shown in figures 7(a) and (b) (the diagrams of (111) and (100) cross sections of the system at 300 K, respectively). The dense regions in which the atoms gather in order and the loose region in which the atoms distribute in disorder can be sharply distinguished. It appears that the icosahedra of (12 0 12 0) and their combining configurations are mainly formed by the 1551 bond type with short-range order. From the size of cluster configurations, the scope of the short-range-order region of the amorphous state must be enlarged with the decrease of temperature. However, in the loose regions, there are indeed some 'vacancies', or 'free volumes', and the sizes of vacancies are also enlarged with the decrease of temperature.

3.3. Transition mechanisms

In order to explain the physical origins of the characteristics mentioned above, it is necessary to understand the relationship between the structural models represented by the HA bond-type index and the typical crystal structures, and the degree of ordering as well.

Firstly, according to the work of Honeycutt and Andersen [23], for a small cluster consisting of 19 atoms, there are three different configurations: an icosahedron, hcp and fcc. They have different binding energies, 3.8242, 3.6342 and 3.6288 (in reduced atomic units). It is well known that the higher the bonding energy, the higher the stability of the cluster. Thus the degree of ordering of the icosahedral cluster would be the highest among these three clusters. Secondly, according to the definitions of HA bond-type index [23], having investigated the relationships between all the structures, represented by the root pairs of atoms and their related near neighbours, and the degree of ordering, we find that the greater the number of atoms involved in a bond type (namely the second number of the HA index), and the greater the number of the near neighbours connected to each other (namely the third number of the HA index), the higher the degree of ordering of the structure involved by the bond type.

Based on the above arguments, we postulate that each structure of all the small clusters (corresponding to some polyhedron) represented by the HA bond-type index will correspond to a certain degree of ordering. For all the bond types in this paper, their degrees of ordering are decreased in the following order: 1661, 1551, 1541, 1441, 1431, 1422, 1421, 1321, 1311, 1211 and 1201. For the clusters mentioned above, the degree of ordering of the icosahedral cluster expressed by (12 0 12 0) in the cluster bond-type index method is one of the highest.

From the present results, we can develop a physical picture of the microstructure transition from liquid to amorphous metal during the rapid cooling process:

With decreasing temperature, the kinetic energy of atoms in the system will be decreased. Thus the probabilities of collision and diffusion of the atoms will also be decreased, and the bond types with a lower degree of ordering will transform into the bond types with a higher degree of ordering [29]. This leads to an important transition from the other bond types to the 1551 bond type with a higher degree of ordering. Thus the degree of ordering of the system is increased continuously. This is simply an expected result according to the thermodynamics theory. Why is this transition not in favour of the 1661 bond type with the highest degree of ordering? We think the main reason is related to dynamic and geometrical factors. The 1661 bond type demands six near-neighbour atoms bonded to each other. The opportunity for atoms to be arranged like this would be less than those for the other bond types. Consequently, the relative number of the 1661 bond type in the system, as shown in table 1, has little change and keeps at 5–6% of the total bond types, and the number of polyhedra containing the 1661 bond type decreases as temperature decreases, as shown in table 2.

With decreasing temperature, 1541 and 1431 are the two main bond types, and their total number has a insignificant change from the liquid to the amorphous state. Moreover, their directions of change are opposite to each other; the total number of the two bond types increases to about 37.3%. In this case, they are in a kinetic equilibrium. This is achieved from the balanced transitions from the 1541 and 1431 bond types to the 1551 bond type with a higher degree of ordering, and from the 1531 and 1421 bond types with a lower degree of ordering to the 1541 and 1431 bond types.

During the formation process of an amorphous metal by rapid cooling, the system goes through the transitions from liquid to supercooled liquid, and finally to the amorphous state. Various polyhedral cluster structures are formed involving various bond types during these transition processes. The icosahedral structure consisting of 1551 bond types with the highest degree of ordering plays an important role in microstructural evolution. New and large clusters can be formed as a result of the combination of various polyhedral cluster structures.

On the other hand, with the rapid decrease of temperature, atoms in or near free states, namely, in the disordered state in the system, will be decreased remarkably, from 12% at 943 K to 7% at 300 K.

4. Conclusions

- Molecular dynamics simulation of the rapid cooling process for a large-scale system of liquid Al metal has been performed, facilitated by parallel computation. It is demonstrated that large clusters can be generated by this simulation method which is more acceptable than the previous studies.
- In addition to the normal HA method, the CBTIM method is presented to describe the configuration of large clusters. The method is shown to be effective in analysing the microstructural evolutions during the rapid cooling process.
- During the rapid cooling process of liquid metal Al, the number of (12 0 12 0) icosahedral clusters consisting of 1551 bond types, with a higher degree of ordering, increases continuously and plays a dominant role in the solidifying transition. Cluster configurations formed by icosahedral clusters and FK, Bernal and defective polyhedra constitute the short-range-order regions in the whole amorphous system, while the atoms not taking part in forming clusters occupy the sparse regions possessing disorder characteristics.
- Large clusters consisting of more than 150 atoms are formed by combining small clusters during the rapid cooling process. The cluster configurations do not have crystal structures of multi-shell configurations formed by octahedral shells produced by gaseous deposition and ionic spray methods.

Acknowledgment

References

[1] Li H, Bian X F and Wang G H 2001 *Mater. Sci. Eng.* A **298** 245
[2] Liu R S *et al* 2001 *Chin. Phys. Lett.* **18** 1383
[3] Liu C S, Zhu Z G, Xia J C and Sun D Y 2000 *Chin. Phys. Lett.* **17** 34
[4] Liu R S *et al* 1999 *Mater. Sci. Eng.* B **57** 214
[5] Li H, Bian X F and Zhang J X 1999 *Mater. Sci. Eng.* A **271** 116
[6] Li J Y *et al* 1998 *J. Mater. Sci. Technol.* **14** 461
[7] Liu R S *et al* 1998 *Trans. Nonferr. Met. Soc. China* **8** 533
[8] Liu R S, Li J Y and Zhou Q Y 1995 *Chin. Sci. Bull.* **40** 1429
[9] Lu J and Szpuner J A 1993 *Acta Metall. Mater.* **41** 2991
[10] Liu R S, Li J Y and Du H Q 1993 *Chin. Sci. Bull.* **38** 1861
[11] Stepanyuk V S *et al* 1992 *J. Non-Cryst. Solids* **151** 169
[12] Liu R S and Wang S 1992 *Phys. Rev.* B **46** 12001
[13] Chatterjee A *et al* 1999 *J. Eur. Ceram. Soc.* **19** 2257
[14] Vashishta P *et al* 1996 *Solid State Mater. Sci.* **1** 853
[15] Kalia R K *et al* 2000 *Comput. Phys. Commun.* **128** 245
[16] Zheng C X *et al* 2001 *Trans. Nonferr. Met. Soc. China* **11** 35
[17] Liu R S *et al* 2002 *Mater. Sci. Eng.* B **94** 141
[18] Dhara S *et al* 2001 *J. Alloys Compounds* **326** 284
[19] Magudapathy P *et al* 2001 *Physica* B **299** 142
[20] Spiridis N, Haber J and Korecki J 2001 *Vacuum* **63** 99
[21] Wang S and Lai S K 1980 *J. Phys. F: Met. Phys.* **10** 2717
[22] Li D H, Li X R and Wang S 1986 *J. Phys. F: Met. Phys.* **16** 309
[23] Honeycutt J D and Andersen H C 1987 *J. Phys. Chem.* **91** 4950
[24] Waseda Y 1980 *The Structure of Non-Crystalline Materials* (New York: McGraw-Hill) p 270
[25] Liu R S, Qi D W and Wang S 1992 *Phys. Rev.* B **45** 451
[26] Qi D W and Wang S 1991 *Phys. Rev.* B **44** 884
[27] Martin T P, Naher U and Schaber H 1992 *Chem. Phys. Lett.* **199** 470
[28] Broyer M 1993 *J. Non-Cryst. Solids* **156–158** 787
[29] Liu R S 1988 *Mater. Sci. Eng.* A **100** L1